AMERICAN SOCIETY FOR MICROBIOLOGY | mSphere®

RESEARCH ARTICLE

Acinetobactin-Mediated Inhibition of Commensal Bacteria by *Acinetobacter baumannii*

Gregory A. Knauf,[a,b] Matthew J. Powers,[c] Carmen M. Herrera,[d] M. Stephen Trent,[c,d] Bryan W. Davies[a,b]

[a]Department of Molecular Biosciences, University of Texas at Austin, Austin, Texas, USA
[b]Center for Systems and Synthetic Biology, John Ring LaMontagne Center for Infectious Diseases, University of Texas at Austin, Austin, Texas, USA
[c]Department of Microbiology, College of Arts and Sciences, University of Georgia, Athens, Georgia, USA
[d]Department of Infectious Diseases, University of Georgia, Athens, Georgia, USA

ABSTRACT *Acinetobacter baumannii* is an important hospital-associated pathogen that causes antibiotic resistant infections and reoccurring hospital outbreaks. *A. baumannii*'s ability to asymptomatically colonize patients is a risk factor for infection and exacerbates its spread. However, there is little information describing the mechanisms it employs to colonize patients. *A. baumannii* often colonizes the upper respiratory tract and skin. Antibiotic use is a risk factor for colonization and infection suggesting that *A. baumannii* likely competes with commensal bacteria to establish a niche. To begin to investigate this possibility, we cocultured *A. baumannii* and commensal bacteria of the upper respiratory tract and skin. In conditions that mimic iron starvation experienced in the host, we observed that *A. baumannii* inhibits *Staphylococcus epidermidis*, *Staphylococcus hominis*, *Staphylococcus haemolyticus* and *Corynebacterium striatum*. Then using an ordered transposon library screen we identified the *A. baumannii* siderophore acinetobactin as the causative agent of the inhibition phenotype. Using mass spectrometry, we show that acinetobactin is released from *A. baumannii* under our coculture conditions and that purified acinetobactin can inhibit *C. striatum* and *S. hominis*. Together our data suggest that acinetobactin may provide a competitive advantage for *A. baumannii* over some respiratory track and skin commensal bacteria and possibly support its ability to colonize patients.

IMPORTANCE The ability of *Acinetobacter baumannii* to asymptomatically colonize patients is a risk factor for infection and exacerbates its clinical spread. However, there is minimal information describing how *A. baumannii* asymptomatically colonizes patients. Here we provide evidence that *A. baumannii* can inhibit the growth of many skin and upper respiratory commensal bacteria through iron competition and identify acinetobactin as the molecule supporting its nutritional advantage. Outcompeting endogenous commensals through iron competition may support the ability of *A. baumannii* to colonize and spread among patients.

KEYWORDS *Acinetobacter*, acinetobactin, iron utilization

The bacterial pathogen, *Acinetobacter baumannii*, is a cause of hospital-associated bacterial disease (1, 2). *A. baumannii* quickly acquires antibiotic resistance, which has led to an increased proportion of multi-drug resistant infections compared with other ESKAPE (*Enterococcus faecium*, *Staphylococcus aureus*, *Klebsiella pneumoniae*, *Acinetobacter baumannii*, *Pseudomonas aeruginosa*, and *Enterobacter* species) pathogens and entry to the CDC urgent threats list for bacteria most in need of new antibiotics (1, 3). Unfortunately, antibiotic development has stagnated (3). This has placed increased pressure on infection prevention to control *A. baumannii*. Environmental contamination (4) and asymptomatic patient colonization are important reservoirs for *A. baumannii* infection in clinical settings (4–20). Additionally, *A. baumannii* colonization is a

Editor Craig D. Ellermeier, University of Iowa

Address correspondence to Bryan W. Davies, bwdavies@austin.utexas.edu.
The authors declare no conflict of interest.
Received 11 January 2022
Accepted 25 January 2022
Published 9 February 2022

major risk factor for future symptomatic *A. baumannii* infections, such as bacteremia and pneumonia, in individual patients (4, 6, 9, 10, 13, 15). Unfortunately, there is a dearth of knowledge relating to the mechanisms by which *A. baumannii* successfully colonizes patients.

In clinical settings, *A. baumannii* is commonly isolated from patient skin at various exposed sites as well as the upper respiratory tract (14–20). Recent antibiotic exposure is an important risk factor for general *A. baumannii* patient colonization (4, 9–11, 18). This suggests that *A. baumannii* competes with the host microbiota to colonize humans. Access to limited nutrients is often a focal point of microbial competition (21–23). A persistently limited resource in the human host is iron. This is due to the human host sequestering iron from bacteria in addition to microbial use of this finite resource (21–23). Under iron limited conditions it has been reported that pathogenic and commensal bacteria can be induced to exhibit competitive behaviors. For example, *Staphylococcus lugdunensis* can inhibit *Staphylococcus aureus* growth under iron limiting conditions via the secretion of the cyclic peptide lugdunin (24, 25) and *Escherichia coli* Nissile decreases *Salmonella enterica* Typhimurium colonization *in vivo* via competition for iron (26).

Here we investigated the ability of *A. baumannii* to compete with commensal bacteria common to the skin and upper respiratory track. We discover that under iron limiting conditions, *A. baumannii* inhibits the growth of common microbiome skin inhabitants *Corynebacterium striatum*, *Staphylococcus epidermidis*, *Staphylococcus hominis* and *Staphylococcus haemolyticus*. Through genetic and biochemical studies, we demonstrate that the *A. baumannii* siderophore acinetobactin is an important factor in this competition. Cumulatively, these data suggest a role for acinetobactin in *A. baumannii* host colonization and commensal competition.

RESULTS

***A. baumannii* inhibits the growth of commensal bacteria under iron limiting conditions.** The microbiome of human skin and upper respiratory tract is less diverse than that of the gastrointestinal tract. *Staphylococcus* spp. and *Corynebacterium* spp. are prominent commensal bacteria of the skin and entire upper respiratory tract that invading pathogens must compete with to establish colonization and or infection (21, 22, 27–32). The localization of these bacteria at these sites suggests the possibility of competition with *A. baumannii*. To begin we selected representative bacteria documented in ATCC (*S. epidermidis* 12228, *S. epidermidis* 35984, *C. striatum* 6940 and *C. propinquum* 51488) and 4 bacterial isolates from the skin and nasal cavity of a healthy human volunteer (two *S. epidermidis* isolates, *S. hominis* and *S. haemolyticus*). We hypothesized that *A. baumannii* may influence the growth of commensal bacteria to promote its own colonization. To test this hypothesis *in vitro* we initially co-plated *A. baumannii* strain 17978 with strains of *S. epidermidis*, *S. hominis*, *S. haemolyticus*, *C. striatum* and *C. propinquum* on nutrient rich medium, but did not observe any effect of *A. baumannii* on the growth of these bacteria (Fig. 1A).

Compared with laboratory medium, the skin and upper respiratory track are nutrient poor niches. Scarce resources have been shown to trigger changes in microbial community dynamics, such as through effector molecules or altered growth through preferential resource acquisition (21–23). Iron is a scarce nutrient that bacteria have been shown to compete for in many niches (21, 23–25, 33). Therefore, we hypothesized that competition between *A. baumannii* and commensal bacteria may also be induced under iron limiting conditions. Iron limitation can be mimicked *in vitro* through the use of the iron chelator 2,2′-dipyridyl. To test this possibility, we repeated co-plating *A. baumannii* strain 17978 with the same set of commensal bacteria. Under iron depleted conditions we observed that *A. baumannii* 17978 inhibited the growth of all of the *Staphylococcus* species and *C. striatum* but, interestingly not *C. propinquum* (Fig. 1A). Furthermore, the strains of *Staphylococcus* species and *C. striatum* had different sensitivities to *A. baumannii* inhibition suggesting variable resistance to *A. baumannii* competition at the strain level (Fig. 1B). To examine the distribution of this

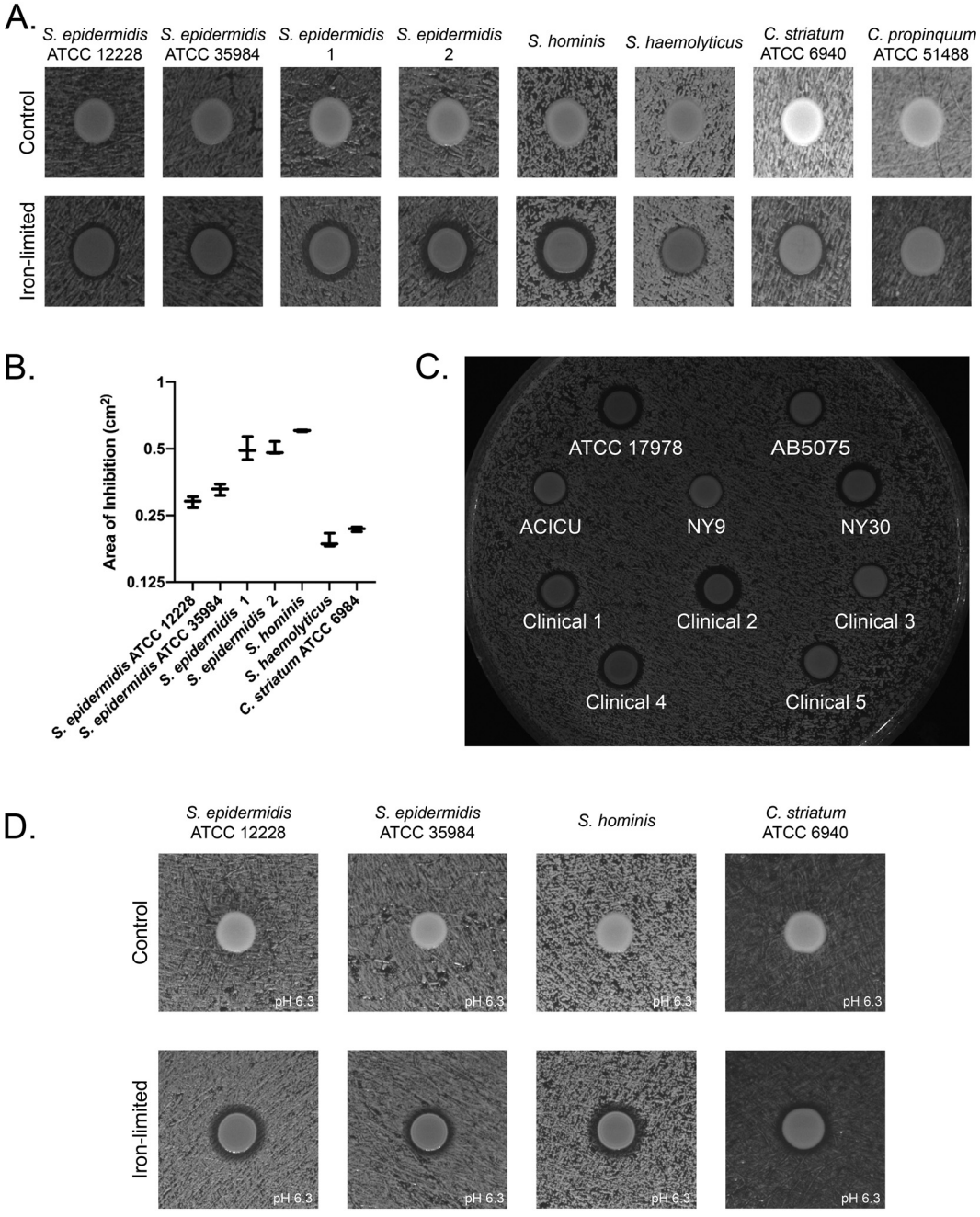

FIG 1 *A. baumannii* inhibits growth of *Staphylococcus* and *Corynebacterium* species under iron-limited conditions. (A) *A. baumannii* 17978 was spotted on a lawn of the indicated *Staphylococcus* or *Corynebacterium* species, grown on nutrient rich agar alone (control) or with 200 μM the iron chelator 2,2′-dipyridyl (Iron limited). *A. baumannii* generated a zone of clearance against all strains except *C. propinquum* ATCC 51488 under iron limited conditions. Experiments were performed in triplicate. A representative image is shown. (B) Quantification of A. $n = 3$ per competition for inhibited bacteria. The error bars represent the standard error of the mean. (C) Multiple laboratory and clinical *A. baumannii* isolates inhibit the growth of *S. hominis* under iron depleted conditions. (D) *A. baumannii* 17978 inhibits representative *Staphylococcus* and *Corynebacterium* species at pH 6.3 (Buffered using 50 mM MES.) in addition to standard culture pH conditions.

phenotype among *A. baumannii* isolates we tested several clinical and laboratory *A. baumannii* strains for the ability to create a zone of inhibition against *S. hominis*. Each *A. baumannii* strain produced a zone of clearance of varying size against *S. hominis* indicating that this phenotype is widespread among *A. baumannii* strains (Fig. 1C).

The pH of the skin and the upper respiratory tract can vary from ~5 to 7 (29, 34, 35). It is known that pH can play an important role in bacterial interactions and growth

TABLE 1 AB5075 Genes with Three or More Transposon Allele Disruptions Resulting in Loss of *S. epidermidis* Inhibition

Locus	Gene name	Putative function
ABUW_0251	–	GNAT domain-containing protein
ABUW_0988	–	putative RNA polymerase Sigma E (40)
ABUW_1169	*basA*	non-ribosomal peptide synthetase
ABUW_1170	*basB*	non-ribosomal peptide synthetase
ABUW_1179	*basD*	nonribosomal peptide synthetase
ABUW_1180	*basE*	2,3-dihydroxybenzoate-AMP ligase
ABUW_1182	*basG*	histidine decarboxylase
ABUW_1176	*bauB*	ferric acinetobactin transport system periplasmic binding protein
ABUW_3120	*bioA*	adenosylmethionine-8-amino-7-oxononanoate transaminase
ABUW_3886	*purE*	phosphoribosylaminoimidazole carboxylase, catalytic subunit
ABUW_1532	*purH*	phosphoribosylaminoimidazolecarboxamide formyltransferase/IMP cyclohydrolase
ABUW_0981	*purM*	phosphoribosylformylglycinamidine cyclo-ligase

(36, 37). This suggests that an *in vivo* relevant pH change may affect the *A. baumannii* inhibitory phenotype since, standard tryptic soy and brain and heart infusion agar is about pH 7.3–7.4. To determine if pH influences competition, we repeated our assays using medium buffered at pH 6.3. Under these conditions we observed the same inhibitory phenotype for *A. baumannii* with regard to a set of representative *S. epidermidis*, *S. hominis*, and *C. striatum* strains (Fig. 1D).

Acinetobactin biosynthesis influences *A. baumannii* commensal inhibition. Zone of inhibition phenotypes regulated by iron concentration have been reported for both siderophores that acquire iron for the secreting organism (38) and secreted antimicrobials that kill competing bacteria (25, 32). To begin investigating genetic factors facilitating *A. baumannii* competition in an unbiased manner, we screened an ordered *A. baumannii* AB5075 transposon (T26) library (39) for reduction in the size of the zones of inhibition with *S. epidermidis* ATCC 12228 under iron limiting conditions. To increase the stringency of our analysis, we filtered the list of potential genes keeping only those for which three or more unique transposon insertions were identified as having a reduced zone of inhibition. This generated a list of 12 genes (Table 1). The genes listed in Table 1 is comprised solely of hits in which three or more different transposon insertion alleles of the same gene were identified in the screen as having a reduced zone of inhibition. Genes encoding the iron siderophore acinetobactin biosynthesis and transport operon represented half of the genes (6/12) in the filtered list. The remaining genes encoded functions associated with purine metabolism, biotin biosynthesis, gene regulation (putative RpoE homologue (40)), and an unknown function. The importance of iron chelation to the inhibitory phenotype *A. baumannii* produces suggests that acinetobactin is a strong candidate for playing an active role in the observed inhibition of *Staphylococcus* species and *C. striatum*.

The acinetobactin biosynthesis pathway has been identified in the *Acinetobacter* genus as a virulence factor important for iron acquisition during infection (41–45). Additionally, acinetobactin is known to be upregulated in iron limiting conditions (46). Interestingly, despite *A. baumannii* AB5075 encoding genes to produce more than one siderophore (42), similar to other *A. baumannii* strains (46), only the acinetobactin siderophore biosynthesis pathway mutants showed decreased inhibition in our screen (Table 1). The loss of an inhibitor zone could be due to either a loss of the inhibitor compound, a reduced growth rate for the *A. baumannii* mutant or both. The growth of each acinetobactin transposon mutant on solid media, the condition used to examine the phenotype of interest, was similar to the parental strain (Fig. 2A). Additionally, the growth rates of the transposon mutants were comparable to the wild-type strain in liquid culture (Fig. 2B). This suggests that the other siderophore systems are sufficient to maintaining growth of AB5075 under our iron limited conditions. To verify the transposon library screen results, we compared wild-type *A. baumannii* AB5075, and transposon mutants *basA*:T26, *basB*:T26, *basD*:T26, *basE*:T26, *basG*:T26, and *bauB*:T26 inhibition of *S. epidermidis* ATCC 12228, ATCC 35984, *S. hominis*, and *C. striatum* ATCC 6940 on

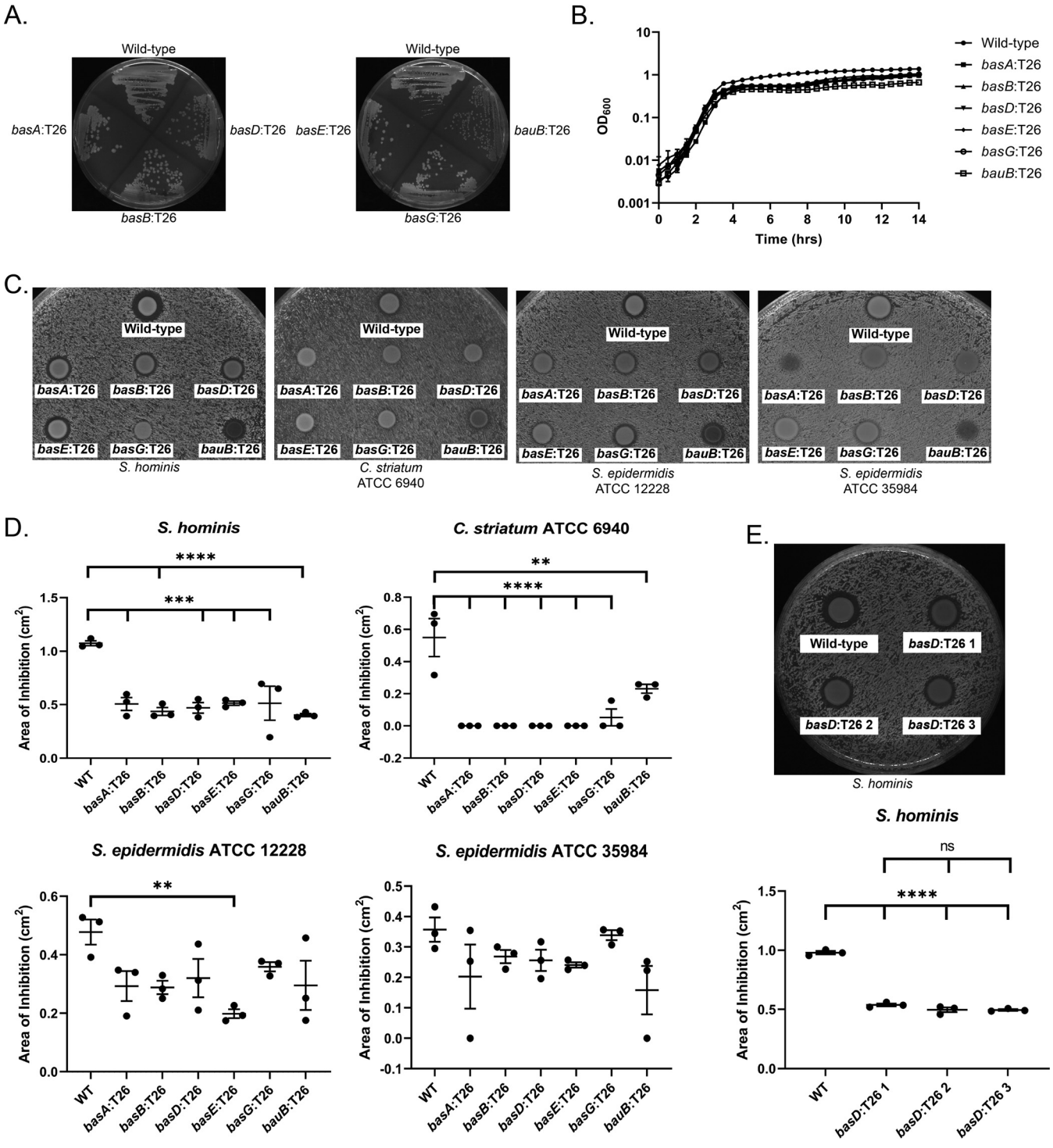

FIG 2 *A. baumannii* AB5075 Acinetobactin mutants exhibit decreased inhibition of multiple bacteria. (A) Growth of the parent and transposon mutant strains of *A. baumannii* AB5075 on 300 μM 2,2′-dipyridyl. (B) Growth curves of wild-type and transposon mutant strains of *A. baumannii* AB5075 grown in 300 μM 2,2′-dipyridyl tryptic soy broth. Growth curves were conducted in triplicate and plotted on a logarithmic scale. The error bars represent the standard error of the mean. (C) *A. baumannii* AB5075 transposon mutant and wild-type zones of inhibitions on iron limited media. Zone of inhibition assays were conducted in triplicate. (D) Quantification of the zones of inhibition in C. The error bars represent the standard error of the mean. An ANOVA with multiple comparisons, comparing each mutant to the control wild-type strain, was used to assess significance. (E) *A. baumannii* AB075 wild-type and three *basD*:T26 isogenic mutant zones of inhibition and quantification. The error bars represent the standard error of the mean. An ANOVA with multiple comparisons was used to assess significance. (**, $P \leq 0.01$; ***, $P \leq 0.001$; ****, $P \leq 0.0001$).

2,2′-dipyridyl medium (Fig. 2C). Our results demonstrate that, compared with the wild type *A. baumannii* 5075 strain, each acinetobactin biosynthesis mutant showed a significant reduction in zone of inhibition against *S. hominis* and *C. striatum* (Fig. 2D). The mean zone of inhibition of each mutant against *S. epidermidis* ATCC 12228 was also smaller compared with the wild-type strain, but only the *basE* mutant showed a statistically significant reduction in zone size. Additionally, mutant zones of inhibition for *S. epidermidis* ATCC 35984 were generally lower than those for the wild-type strain, but none were statistically significant. These results highlight that the importance of acinetobactin for *A. baumannii* competition will likely vary with the competing bacteria. Some mutants (*basA*, *bauB*) also showed variations in growth when cocultured with different bacteria under iron limited conditions. While the reason for this is unclear and could be the result of numerous possible causes, this phenotype appeared in each replicate of the experiments. The residual zone of clearance around some of the transposon mutants observed with *S. epidermidis* (12228 and 35984) and *S. hominis* suggests *A. baumannii* AB5075 may have additional factors it employs for competition under iron limited conditions.

In sum, our genetic data suggests that acinetobactin plays an important role in interactions between *A. baumannii* and nasal and skin commensals. The structure and size of the acinetobactin biosynthesis operon negates simple complementation. However, identifying multiple Tn mutants in strain AB5075 all clustering in the acinetobactin biosynthesis pathway, and influencing inhibition of nasal and skin commensals (Fig. 2C), supports an important role for acinetobactin in *A. baumannii* competition. Furthermore, we tested three separate transposon insertion mutants of *basD* identified in the transposon library screen and found similar inhibition for the three isogenic mutants when tested in triplicate for zones of inhibition against *S. hominis* (Fig. 2E). To provide direct evidence for acinetobactin in commensal inhibition we proceeded to biochemical studies.

***A. baumannii* produces acinetobactin during competition under iron-limited conditions.** Up to this point, our genetic results indicate that acinetobactin biosynthesis is important for the *in vitro* inhibition of Staphylococcal species and *C. striatum*. However, this does not demonstrate that acinetobactin is actually produced or present when commensal bacteria are inhibited. To address this, we first demonstrated that acinetobactin could be isolated from wild-type *A. baumannii* and second, we used MALDI-IMS (MALDI Imaging Mass Spec) to further investigate the production of acinetobactin and its correlation with inhibition of commensals using *S. epidermidis* as the test case.

We began by isolating acinetobactin from wild-type *A. baumannii* ATCC 17978 as previously described (47). *A. baumannii* was grown for 48 h in 1 liter of M9 minimal media with succinate as the carbon source. Acinetobactin was isolated from the supernatant via XAD-7HP resin and preparatory HPLC followed by lyophilization to obtain the crude product mass. The lyophilized product was then rehydrated with sterile deionized water. The presence of acinetobactin was confirmed by mass spectrometry. The high-resolution spectra observed for monoisotopic acinetobactin in our preparation is shown in Fig. 3A. The observed *m/z* matches the theoretical *m/z* of acinetobactin. This demonstrates that our *A. baumannii* ATCC 17978 strain can produce acinetobactin and we successfully isolated a crude product containing acinetobactin.

MALDI-TOF mass spectrometry imaging allows for the determination of molecule production and location in two-dimensional space. We observed that only when grown in iron-limited conditions did the *A. baumannii* 17978 parental strain noticeably produce acinetobactin that diffuses into the *S. epidermidis* lawn (Fig. 3B). Importantly, acinetobactin appears to be dispersed throughout the zone of inhibition as would be expected for a secreted factor. This is an important finding since, if acinetobactin was capable of inhibiting some species of bacteria it should be present where the inhibition is taking place.

Purified acinetobactin inhibits commensal bacteria growth. The circumstantial evidence that acinetobactin can inhibit some species *in vitro* produced through the

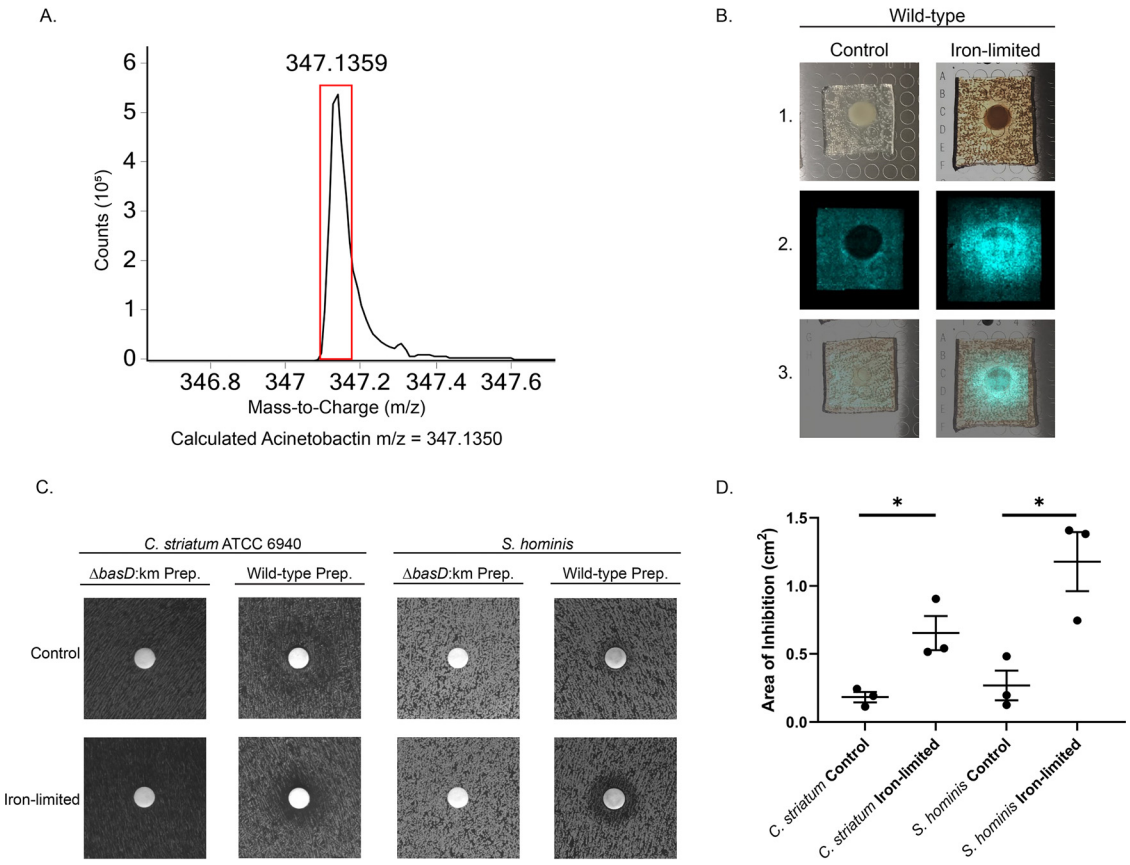

FIG 3 Biochemical evidence for acinetobactin-mediated inhibition. (A) Accurate mass spectra of the monoisotopic peak for acinetobactin preps purified from wild-type *A. baumannii* ATCC 17978. The red box represents where the peak is expected to be for acinetobactin. The theoretical *m/z* of monoisotopic acinetobactin is 347.1350, error 2.5 ppm and the observed *m/z* was 347.1359. (B) MALDI-IMS of acinetobactin production. 1. Images of wild-type 17978 spotted on a lawn of *S. epidermidis* 12228 on medium with (iron-limited) or without (control) 2,2′-dypyridyl. 2. Mass spectrometry analysis of the presence of acinetobactin. Presence of acinetobactin is false colored blue. 3. Overlap of 1 and 2. Experiments were repeated in triplicate and a representative image is shown. (C) HPLC prepped acinetobactin was added to a filter disk on a lawn of *C. striatum* or *S. hominis* on either 200 μM or 0 μM 2,2′-dypyridyl. A zone of inhibition indicates growth inhibition. Experiments were replicated and a representative image is shown. HPLC preps from a *basD*:km mutant was used as the control for inhibitory activity. (D) Quantification of the zones of inhibition for wild-type preps in C. The mean and standard error of the mean is shown in addition to the individual measurements. Significance was tested using a paired T-test comparing the control and iron-limited samples for each bacterial species. (**, $P \leq 0.05$).

use of MALDI-TOF mass spectrometry is compelling. However, it is still indirect evidence. To directly determine whether acinetobactin can inhibit bacteria *in vitro*, we used purified acinetobactin and an identical preparation from a 17978 *basD*:km mutant culture. We selected theses strains as 17978 has a well-defined iron acquisition system including, acinetobactin, and is genetically tractable for producing whole gene deletions. We performed a disc diffusion assay of isolated acinetobactin and a *basD*:km control on *S. hominis* and *C. striatum* grown on iron-limited media and control media. For this assay, we plated the species described and applied a single dose of 500 mg of crude acinetobactin HPLC product, or a *basD*:km control preparation following the same protocol, to the diffusion disc before incubating overnight at 37°C. This assay showed that purified acinetobactin can form a zone of inhibition against *C. striatum* and *S. hominis* (Fig. 3C). These data demonstrate that acinetobactin can inhibit *S. hominis* and *C. striatum* in an iron-dependent manner. These zones of inhibition were quantified and show a significant difference in acinetobactin inhibition between the control and iron-limited conditions (Fig. 3D). These biochemical results further support our genetic analysis indicating that acinetobactin helps *A. baumannii* to inhibit the growth of nasal and skin commensals.

DISCUSSION

Differences in siderophore production among closely related species might impact their susceptibility to *A. baumannii* inhibition in this study. For example, our data shows that *C. propinquum*, a species that likely inhibits coagulase negative *staphylococcus* through siderophore production (38), is resistant to *A. baumannii* inhibition compared with *C. striatum*. This suggests that the propensity of *A. baumannii* to establish itself in a microbiome may be variable between different host microbiomes in part as a function of iron acquisition capabilities. This is further suggested by the strain level variation in zones of inhibition depending on the *S. epidermidis* strain. This deserves further investigation to fully understand the role of iron competition in *A. baumannii* colonization.

Acinetobactin biosynthesis is a widely distributed capability of *A. baumannii* strains (42, 45, 46). Additionally, acinetobactin can bind iron in a wide range of pHs present in many different niches in the human body (47). Therefore, based off our results, we believe acinetobactin may play a major role in the success of *A. baumannii* in the human body in colonization in addition to its known importance in infection. While the *A. baumannii* AB5075 acinetobactin biosynthesis mutants exhibited decreased inhibition, the inhibition was not fully eliminated for all bacteria tested here. It is known that different *A. baumannii* strains are often capable of producing additional siderophores (42, 46). This suggests that in AB5075 the other siderophores may play a role in commensal inhibition despite our transposon library results only suggesting acinetobactin. To determine the ultimate extent of acinetobactin's role in these processes other siderophores in *A. baumannii*'s arsenal should be explicitly investigated for a role in colonization and commensal competition.

While the *in vitro* inhibition experiments in this study focused on representative bacterial species of the upper respiratory and skin it is not clear how the same pairwise interactions would play out *in vivo*. Beyond these types of pairwise competitions, it is even less clear how the multi-domain web of interactions that take place *in vivo* may or may not impact *A. baumannii* colonization such as the metabolic capabilities, biofilm formation, resistance and/or manipulation of host defense factors and growth rates of *A. baumannii* strains and commensal microorganisms.

Through the experiments described here we have begun to investigate a possible role for acinetobactin in competition for iron in *A. baumannii* colonization. Given the importance of iron acquisition to survival in the microbiome, we expect that these experiments will be able to provide orientation for additional studies of host colonization more broadly. Finally, these data suggest a potential route to target *A. baumannii* to reduce the risk of *A. baumannii* spread and infection. This could potentially be done using antibiotic-siderophore conjugates as an approach that may prove fruitful in decolonization of patients in medium to long-term medical settings resulting in improved infection control. This study also suggests that commensal bacteria resistant to *A. baumannii* iron competition could offer an additional option for *A. baumannii* infection prevention or treatment.

MATERIALS AND METHODS

Isolation and Identification of Bacterial Species. Bacterial isolates were isolated by swabbing the anterior nares, back and forehead of a healthy volunteer. These samples were then streaked on tripticase-soy agar and allowed to grow for 48 h at 30°C. Single colonies were then streaked and grown on new plates to ensure the isolation of individual species. Then frozen stocks were prepared for each selected isolate. Isolates were then subjected to 16S amplicon sequencing using the 27F-HT/1492R-HT primer pair (48) for PCR amplification.

Zone of Inhibition Assays. Zone of inhibition assays were carried out using Tripticase-soy media for *Staphylococcus* species and Brain and Heart Infusion media for Corynebacterium species 7.5 g of agar was added to 500 mL of growth media to form solid media. 2,2′-dipyridyl was added to media at the specified concentrations after being dissolved in dimethyl sulfoxide. 2,2′-dipyridyl was used at 200 μM for *A. baumannii* 17978 zones of inhibition, the transposon library screen, and when comparing the zones of inhibition formed by multiple *A. baumannii* isolates. Three hundred micometers of 2,2′-dipyridyl was used for assessing *A. baumannii* AB5075 transposon mutant zones of inhibition compared with the parental strain. Then 100 μL of the described bacteria at an OD_{600} ~0.005, diluted in phosphate-buffered

TABLE 2 Strains utilized

Strain name	Source
A. baumannii 17978 wild type	ATCC
A. baumannii 17978 *basD* deletion	This study
A. baumannii AB5075 wild type	Gallagher et al. (2015) (39)
A. baumannii AB5075 *bauB* transposon mutant, tnab1_kr121127p08q178	Gallagher et al. (2015) (39)
A. baumannii AB5075 *basA* transposon mutant, tnab1_kr121203p08q104	Gallagher et al. (2015) (39)
A. baumannii AB5075 *basG* transposon mutant, tnab1_kr130909p02q141	Gallagher et al. (2015) (39)
A. baumannii AB5075 *basB* transposon mutant, tnab1_kr130913p04q187	Gallagher et al. (2015) (39)
A. baumannii AB5075 *basE* transposon mutant, tnab1_kr130916p02q117	Gallagher et al. (2015) (39)
A. baumannii AB5075 *basD* transposon mutant, tnab1_kr130917p06q182	Gallagher et al. (2015) (39)
A. baumannii AB5075 *basD* transposon mutant, tnab1_kr130913p06q115	Gallagher et al. (2015) (39)
A. baumannii AB5075 *basD* transposon mutant, tnab1_kr130916p05q121	Gallagher et al. (2015) (39)
A. baumannii NY9	Bratu et al. (2008) (50)
A. baumannii NY30	Bratu et al. (2008) (50)
A. baumannii ACICU	Iacono et al. (2008) (51)
A. baumannii Clinical 1	Centre Hospitalier Universitaire de Caen
A. baumannii Clinical 2	Centre Hospitalier Universitaire de Caen
A. baumannii Clinical 3	Centre Hospitalier Universitaire de Caen
A. baumannii Clinical 4	Centre Hospitalier Universitaire de Caen
A. baumannii Clinical 5	Centre Hospitalier Universitaire de Caen
S. epidermidis 12228	ATCC
S. epidermidis 35984	ATCC
S. epidermidis 1	This study
S. epidermidis 2	This study
S. hominis	This study
S. haemolyticus	This study
C. striatum 6940	ATCC
C. propinquum 51488	ATCC

saline (PBS), was spread on the plate using glass beads to form a bacterial lawn. Then 10 μL of *A. baumannii* at an OD_{600} ~1.0 was spotted on the plate and allowed to dry. Following, the spotting of *A. baumannii* the plate was incubated at 37°C overnight. When making dilutions of either *A. baumannii* or the species to be inhibited bacteria were grown overnight at 37 degrees on solid media then colonies were suspended to the correct optical density in PBS.

Where images are cropped to show a single zone of inhibition that zone of inhibition is the only zone of inhibition on a plate. When multiple zones of inhibition are performed on the same plate to compare inhibiting strains all strains tested are shown. Larger plates (150 × 22 mm) were used when more than four inhibiting strains were compared. In this circumstance the volume of inhibited bacteria was increased in proportion to the change in the size of the plate compared with plates used otherwise.

Measurements of the area of inhibition were performed in triplicate with a known scale for measurements included in each image. The measurements were performed using ImageJ. To acquire the area of the zone of inhibition, the area of only the *A. baumannii* spot was subtracted from that of the inhibition area and spot.

Transposon Library Screen. The transposon library was carried out on solid Tripticase-soy agar plates containing 200 μM 2,2′-dipyridyl. First a lawn of *S. epidermidis* ATCC 35984 was plated with 200 μL at 0.005 OD600. Then 96-well plates containing the ordered Three Allele *A. baumannii* AB5075 Transposon Library (39) were thawed and spotted onto the plates using a V&P 96-well replicater (VP 407, 1.5 μL transfer) and allowed to dry. This was carried out for all plates in the library. The plates were incubated overnight at 37°C. The following day colonies of *A. baumannii* AB5075 with a decreased or absence of a zone of inhibition were recorded and identified based on their position within a given 96-well plate. Select transposon mutants were then PCR verified and sanger sequenced.

Genetic Manipulations and Fitness Assays. Gene deletion and complementation was carried out as previously described (49) with single colony isolation carried out on tripticase-soy media.

For liquid growth curves *A. baumannii* strains were grown overnight at 37°C on tripticase-soy agar containing the appropriate antibiotic. Colonies were then suspended in tripticase-soy media to ~0.005 OD_{600} before allocation into a 96-well plate in triplicate. A 14-h growth curve at 37°C with continuous shaking with reads every 15 min in a SpectraMax Plus 384 spectrometer. When plotting every half hour time point was plotted as an average with standard error of the mean error bars.

When streaking bacterial strains for growth assessment on tripticase-soy plates with 0 or 200 μM 2,2′-dipyridyl were prepared. Then, the plates were divided into quadrants and mutant and wild-type strains were streaked from frozen stocks from the outer edge toward the middle. Wild-type *A. baumannii* was streaked on each plate as a control.

MALDI-IMS (MALDI Imaging Mass Spec). Cultures of *A. baumannii* and *S. epidermidis* were normalized to an OD of 0.5 and 0.005 respectively. Microcolony lawns of *S. epidermidis* were spread on 10 mL LB plates with or without 100 μM 2,2′-dipyridyl. After plates were dried, 2.5 μL of the appropriate *A.*

TABLE 3 Primers and plasmids utilized

Name	Source	Primer sequence
A1S_2382-3 recombine F	This study	GACGGACAAGCTATATATTCACAGCAAAATTGGAAATGATTAACAAATGCAACTG GTAATCATTTTCATTTGTTTGTATGATGCTGAAACAAGATTAA TTTGTCAACCGAGTTATCGTTCACCGGAATTGCCAGCTGGG
A1S_2382-3 recombine R	This study	GATGAGACAAAAGAGCAGCTAAACCTAAGTTGAATGGCCCAATACCAATTCCGGT AATATCTATTTTTTTCATGTTTATACTTTATCTGTTTCCAAAATG ATGAAAGTTCAAAATACGAATTCAGAAGAACTCGTCAAG
A1S_2382-3 screen F	This study	CTTGGTAAATTTTCTTACATATCGGCATA
A1S_2382-3 screen R	This study	CTGGTTTACGTTCTAAAAATACGC
AB5075_basA_screen	This study	CGAATCTCCCACCTCAGCTACTGC
AB5075_basB_screen	This study	CTCCATCTGCTGCCGATTTAGCTC
AB5075_basD_screen	This study	CCGGTGAGAGCTGAATCGCGTATGTTTC
AB5075_basE_screen	This study	GGTATAAGGCCCCCGAGTCGC
AB5075_basG_screen	This study	CCATATGGTGTAAGGTTGCGATATCGTC
AB5075_bauB_screen	This study	CCTACAGGTCAGGTGACGTCACTC
TN 26 seq primer Pgro-172	Gallagher et al. (2015) (39)	TGAGCTTTTTAGCTCGACTAATCCAT
27F-HT	Tyson et al. (2004) (48)	AGRGTTTGATYMTGGCTCAG
1492R-HT	Tyson et al. (2004) (48)	GGYTACCTTGTTACGACTT

baumannii strain were spotted. Plates were incubated overnight. The following day, agar was excised and laid onto a coarse ground MALDI target plate (Bruker). The target plate was coated with a 25 mg/mL ATT matrix in 50% Acetonitrile + 0.1% TFA using a HTX TM-Sprayer at a flow rate of 0.2 mL/min. Samples were subsequently imaged by a MALDI Autoflex Speed (Bruker) in reflectron positive mode. Data were analyzed using flexImaging (Bruker) and images generated by false coloring based on spectral intensity.

Purification of Acinetobactin. Acinetobactin was purified as previously described (47). *A. baumannii* 17978 wild-type and *basD*:km strains were grown for 48 h in 1L of M9 minimal media with succinate as the carbon source. Then the supernatant was reserved following centrifugation and adjusted to pH 6.0 using concentrated citric acid. Following pH adjustment, 25g of Amberlite XAD-7 resin was added to the supernatant and placed on an orbital shaker for 4 h at 100 rpm and room temperature. Then the resin was filtered and washed 4 times with de ionized water methanol extraction using a total volume of 1.1 L. The methanol was rotovaped to concentrate the solution for HPLC use. A HPLC gradient of 5% to 95% solvent B over 45 min with, an acinetobactin formic acid salt elution time at ~21 min. Samples were lyophilized to obtain product mass collected. Following rehydration with sterile deionized water Agilent Technologies 6546 Accurate-Mass Q-TOF LC/MS was used to verify the presence of acinetobactin in the collected fractions from wild-type cultures and the absence of acinetobactin in the collected fractions from *basD*:km mutant cultures.

Purified Acinetobactin Zones of Inhibition. Lyophilized HPLC preps from the same elution time point for wild-type and Δ*basD*:km strain cultures were suspended to the same volume using deionized water. *C. striatum* and *S. hominis* were streaked from frozen stocks and grown overnight at 37°C. Control (0 μM 2,2′-dipyridyl) and iron-limited (200 μM 2,2′-dipyridyl) media was prepared for each strain. Each bacterial strain was scraped from the overnight plate and diluted in PBS to an optical density of 0.005. Then 100 μL of each bacterial suspension was plated on each respective agar plate. The diffusion disc was added to the center of each plate and approximately 500 μg of wild-type crude product was added to the diffusion discs for the wild-type preps. An equivalent volume of Δ*basD*:km crude product prep as the wild-type prep was used as the ΔbasD:km prep to control for contaminants affecting bacterial growth. Images were quantified by subtracting the area of the disc from the area of the zones of inhibition using Image J.

Strains, primers, and plasmids. The strains, primers, and plasmids utilized are listed in Tables 2 and 3.

Data availability. All data are available upon request.

ACKNOWLEDGMENTS

This research was supported by National Institutes of Health (R01 AI125337, R01 AI148419, R21 AI159203 to B.W.D.; R01 AI150098, R01 AI129940, R01 AI138576 to MST), and Tito's Handmade Vodka (to B.W.D.). The funders had no role in the study design, data collection and interpretation, or the decision to submit the work for publication.

M.J.P. performed and analyzed data related to MALDI-IMS. CMH assisted with the transposon library screen. The University of Texas at Austin Mass Spectrometry Facility performed accurate mass measurements for acinetobactin. G.A.K. performed all other experiments, data interpretation, figure creation, and writing with guidance from B.W.D. All authors read and approved the final manuscript. We thank the Anslyn

Research Group at The University of Texas at Austin for providing access to their preparatory HPLC.

REFERENCES

1. Centers for Disease Control and Prevention. 2019. Antibiotic resistance threats in the United States, 2019. Centers for Disease Control and Prevention.
2. Dijkshoorn L, Nemec A, Seifert H. 2007. An increasing threat in hospitals: multidrug-resistant Acinetobacter baumannii. Nat Rev Microbiol 5:939–951. https://doi.org/10.1038/nrmicro1789.
3. Oliveira DMPD, Forde BM, Kidd TJ, Harris PNA, Schembri MA, Beatson SA, Paterson DL, Walker MJ. 2020. Antimicrobial eesistance in ESKAPE pathogens. Clin Microbiol Rev 33. https://doi.org/10.1128/CMR.00181-19.
4. Fournier PE, Richet H, Weinstein RA. 2006. The epidemiology and control of Acinetobacter baumannii in health care facilities. Clin Infect Dis 42:692–699. https://doi.org/10.1086/500202.
5. Peleg AY, Seifert H, Paterson DL. 2008. Acinetobacter baumannii: Emergence of a Successful Pathogen. Clin Microbiol Rev 21:538–582. https://doi.org/10.1128/CMR.00058-07.
6. Wenzler E, Goff DA, Humphries R, Goldstein EJC. 2017. Anticipating the unpredictable: a review of antimicrobial stewardship and Acinetobacter infections. Infect Dis Ther 6:149–172. https://doi.org/10.1007/s40121-017-0149-y.
7. Seifert H, Dijkshoorn L, Gerner-Smidt P, Pelzer N, Tjernberg I, Vaneechoutte M. 1997. Distribution of Acinetobacter species on human skin: comparison of phenotypic and genotypic identification methods. J Clin Microbiol 35:2819–2825. https://doi.org/10.1128/jcm.35.11.2819-2825.1997.
8. Zollner-Schwetz I, Zechner E, Ullrich E, Luxner J, Pux C, Pichler G, Schippinger W, Krause R, Leitner E. 2017. Colonization of long term care facility patients with MDR-Gram-negatives during an Acinetobacter baumannii outbreak. Antimicrob Resist Infect Control 6:49. https://doi.org/10.1186/s13756-017-0209-9.
9. Arvaniti K, Lathyris D, Ruimy R, Haidich A-B, Koulourida V, Nikolaidis P, Matamis D, Miyakis S. 2012. The importance of colonization pressure in multiresistant Acinetobacter baumannii acquisition in a Greek intensive care unit. Crit Care 16:R102. https://doi.org/10.1186/cc11383.
10. Corbella X, Montero A, Pujol M, Domínguez MA, Ayats J, Argerich MJ, Garrigosa F, Ariza J, Gudiol F. 2000. Emergence and rapid spread of carbapenem resistance during a large and sustained hospital outbreak of multiresistant Acinetobacter baumannii. J Clin Microbiol 38:4086–4095. https://doi.org/10.1128/JCM.38.11.4086-4095.2000.
11. Playford EG, Craig JC, Iredell JR. 2007. Carbapenem-resistant Acinetobacter baumannii in intensive care unit patients: risk factors for acquisition, infection and their consequences. J Hosp Infect 65:204–211. https://doi.org/10.1016/j.jhin.2006.11.010.
12. Köck R, Werner P, Friedrich AW, Fegeler C, Becker K, Prevalence of Multiresistant Microorganisms PMM Study Group. 2016. Persistence of nasal colonization with human pathogenic bacteria and associated antimicrobial resistance in the German general population. New Microbes New Infect 9:24–34. https://doi.org/10.1016/j.nmni.2015.11.004.
13. García-Garmendia J-L, Ortiz-Leyba C, Garnacho-Montero J, Jiménez-Jiménez F-J, Pérez-Paredes C, Barrero-Almodóvar AE, Miner MG. 2001. Risk factors for Acinetobacter baumannii nosocomial bacteremia in critically ill patients: a cohort study. Clin Infect Dis 33:939–946. https://doi.org/10.1086/322584.
14. Damaceno Q, Nicoli JR, Oliveira A. 2015. Variability of cutaneous and nasal population levels between patients colonized and infected by multidrug-resistant bacteria in two Brazilian intensive care units. SAGE Open Med 3. https://doi.org/10.1177/2050312114566668.
15. Liou M-L, Chen K-H, Yeh H-L, Lai C-Y, Chen C-H. 2017. Persistent nasal carriers of Acinetobacter baumannii in long-term-care facilities. Am J Infect Control 45:723–727. https://doi.org/10.1016/j.ajic.2017.02.005.
16. Vos DD, Pirnay J-P, Bilocq F, Jennes S, Verbeken G, Rose T, Keersebilck E, Bosmans P, Pieters T, Hing M, Heuninckx W, Pauw FD, Soentjens P, Merabishvili M, Deschaght P, Vaneechoutte M, Bogaerts P, Glupczynski Y, Pot B, van der Reijden TJ, Dijkshoorn L. 2016. Molecular epidemiology and clinical impact of acinetobacter calcoaceticus-baumannii complex in a belgian burn wound center. PLoS One 11:e0156237. https://doi.org/10.1371/journal.pone.0156237.
17. Marchaim D, Navon-Venezia S, Schwartz D, Tarabeia J, Fefer I, Schwaber MJ, Carmeli Y. 2007. Surveillance cultures and duration of carriage of multidrug-resistant Acinetobacter baumannii. J Clin Microbiol 45:1551–1555. https://doi.org/10.1128/JCM.02424-06.
18. Wendel AF, Malecki M, Otchwemah R, Tellez-Castillo CJ, Sakka SG, Mattner F. 2018. One-year molecular surveillance of carbapenem-susceptible A. baumannii on a German intensive care unit: diversity or clonality. Antimicrob Resist Infect Control 7:145. https://doi.org/10.1186/s13756-018-0436-8.
19. Kim H-S, Lee SS, Lee J, Kim J-S. 2015. Comparison of methods for surveillance culture of carbapenem-resistant Acinetobacter baumannii. Open Forum Infect Dis 2.
20. Dedeić-Ljubović A, Hukić M. 2012. Occurrence of colonization and infection with multidrug-resistant organisms in a neonatal intensive care unit. Med Glas (Zenica) 9:304–310.
21. Kamada N, Chen GY, Inohara N, Núñez G. 2013. Control of pathogens and pathobionts by the gut microbiota. Nat Immunol 14:685–690. https://doi.org/10.1038/ni.2608.
22. Libertucci J, Young VB. 2019. The role of the microbiota in infectious diseases. Nat Microbiol 4:35–45. https://doi.org/10.1038/s41564-018-0278-4.
23. Hibbing ME, Fuqua C, Parsek MR, Peterson SB. 2010. Bacterial competition: surviving and thriving in the microbial jungle. Nat Rev Microbiol 8:15–25. https://doi.org/10.1038/nrmicro2259.
24. Mashburn LM, Jett AM, Akins DR, Whiteley M. 2005. Staphylococcus aureus Serves as an Iron Source for Pseudomonas aeruginosa during In Vivo Coculture. J Bacteriol 187:554–566. https://doi.org/10.1128/JB.187.2.554-566.2005.
25. Zipperer A, Konnerth MC, Laux C, Berscheid A, Janek D, Weidenmaier C, Burian M, Schilling NA, Slavetinsky C, Marschal M, Willmann M, Kalbacher H, Schittek B, Brötz-Oesterhelt H, Grond S, Peschel A, Krismer B. 2016. Human commensals producing a novel antibiotic impair pathogen colonization. Nature 535:511–516. https://doi.org/10.1038/nature18634.
26. Deriu E, Liu JZ, Pezeshki M, Edwards RA, Ochoa RJ, Contreras H, Libby SJ, Fang FC, Raffatellu M. 2013. Probiotic bacteria reduce salmonella typhimurium intestinal colonization by competing for iron. Cell Host Microbe 14:26–37. https://doi.org/10.1016/j.chom.2013.06.007.
27. Brugger SD, Bomar L, Lemon KP. 2016. Commensal–pathogen interactions along the human nasal passages. PLoS Pathog 12:e1005633. https://doi.org/10.1371/journal.ppat.1005633.
28. Yan M, Pamp SJ, Fukuyama J, Hwang PH, Cho D-Y, Holmes S, Relman DA. 2013. Nasal microenvironments and interspecific interactions influence nasal microbiota complexity and S. aureus carriage. Cell Host Microbe 14:631–640. https://doi.org/10.1016/j.chom.2013.11.005.
29. Man WH, de Steenhuijsen Piters WAA, Bogaert D. 2017. The microbiota of the respiratory tract: gatekeeper to respiratory health. Nat Rev Microbiol 15:259–270. https://doi.org/10.1038/nrmicro.2017.14.
30. Iwase T, Uehara Y, Shinji H, Tajima A, Seo H, Takada K, Agata T, Mizunoe Y. 2010. Staphylococcus epidermidis Esp inhibits Staphylococcus aureus biofilm formation and nasal colonization. Nature; London 465:346–349. https://doi.org/10.1038/nature09074.
31. Byrd AL, Belkaid Y, Segre JA. 2018. The human skin microbiome. 3. Nat Rev Microbiol 16:143–155. https://doi.org/10.1038/nrmicro.2017.157.
32. Janek D, Zipperer A, Kulik A, Krismer B, Peschel A. 2016. High frequency and diversity of antimicrobial activities produced by nasal staphylococcus strains against bacterial competitors. PLoS Pathog 12:e1005812. https://doi.org/10.1371/journal.ppat.1005812.
33. Skaar EP. 2010. The battle for iron between bacterial pathogens and their vertebrate hosts. PLoS Pathog 6:e1000949. https://doi.org/10.1371/journal.ppat.1000949.
34. Roth RR, James WD. 1988. Microbial ecology of the skin. Annu Rev Microbiol 42:441–464. https://doi.org/10.1146/annurev.mi.42.100188.002301.
35. Elias PM. 2007. The skin barrier as an innate immune element. Semin Immunopathol 29:3–14. https://doi.org/10.1007/s00281-007-0060-9.
36. Ratzke C, Gore J. 2018. Modifying and reacting to the environmental pH can drive bacterial interactions. PLoS Biol 16:e2004248. https://doi.org/10.1371/journal.pbio.2004248.
37. Zhou J, Jiang N, Wang Z, Li L, Zhang J, Ma R, Nie H, Li Z. 2017. Influences of pH and iron concentration on the salivary microbiome in individual humans with and without caries. Appl Environ Microbiol 83. https://doi.org/10.1128/AEM.02412-16.

38. Stubbendieck RM, May DS, Chevrette MG, Temkin MI, Wendt-Pienkowski E, Cagnazzo J, Carlson CM, Gern JE, Currie CR. 2019. Competition among nasal bacteria suggests a role for siderophore-mediated interactions in shaping the human nasal microbiota. Appl Environ Microbiol 85. https://doi.org/10.1128/AEM.02406-18.
39. Gallagher LA, Ramage E, Weiss EJ, Radey M, Hayden HS, Held KG, Huse HK, Zurawski DV, Brittnacher MJ, Manoil C. 2015. Resources for genetic and genomic analysis of emerging pathogen Acinetobacter baumannii. J Bacteriol 197:2027–2035. https://doi.org/10.1128/JB.00131-15.
40. Casella LG, Weiss A, Pérez-Rueda E, Antonio Ibarra J, Shaw LN. 2017. Towards the complete proteinaceous regulome of Acinetobacter baumannii. Microb Genom 3.
41. Peleg AY, de Breij A, Adams MD, Cerqueira GM, Mocali S, Galardini M, Nibbering PH, Earl AM, Ward DV, Paterson DL, Seifert H, Dijkshoorn L. 2012. The success of Acinetobacter species; genetic, metabolic and virulence attributes. PLoS One 7:e46984. https://doi.org/10.1371/journal.pone.0046984.
42. Sheldon JR, Skaar EP. 2020. Acinetobacter baumannii can use multiple siderophores for iron acquisition, but only acinetobactin is required for virulence. PLoS Pathog 16:e1008995. https://doi.org/10.1371/journal.ppat.1008995.
43. Yamamoto S, Okujo N, Sakakibara Y. 1994. Isolation and structure elucidation of acinetobactin., a novel siderophore from Acinetobacter baumannii. Arch Microbiol 162:249–254.
44. Penwell WF, Arivett BA, Actis LA. 2012. The Acinetobacter baumannii entA gene located outside the acinetobactin cluster is critical for siderophore production, iron acquisition and virulence. PLoS One 7:e36493. https://doi.org/10.1371/journal.pone.0036493.
45. Antunes LCS, Imperi F, Towner KJ, Visca P. 2011. Genome-assisted identification of putative iron-utilization genes in Acinetobacter baumannii and their distribution among a genotypically diverse collection of clinical isolates. Res Microbiol 162:279–284. https://doi.org/10.1016/j.resmic.2010.10.010.
46. Eijkelkamp BA, Hassan KA, Paulsen IT, Brown MH. 2011. Investigation of the human pathogen Acinetobacter baumannii under iron limiting conditions. BMC Genomics 12:126. https://doi.org/10.1186/1471-2164-12-126.
47. Shapiro JA, Wencewicz TA. 2016. Acinetobactin Isomerization Enables Adaptive Iron Acquisition in Acinetobacter baumannii through pH-Triggered Siderophore Swapping. ACS Infect Dis 2:157–168. https://doi.org/10.1021/acsinfecdis.5b00145.
48. Tyson GW, Chapman J, Hugenholtz P, Allen EE, Ram RJ, Richardson PM, Solovyev VV, Rubin EM, Rokhsar DS, Banfield JF. 2004. Community structure and metabolism through reconstruction of microbial genomes from the environment. Nature 428:37–43. https://doi.org/10.1038/nature02340.
49. Tucker AT, Nowicki EM, Boll JM, Knauf GA, Burdis NC, Trent MS, Davies BW. 2014. Defining gene-phenotype relationships in Acinetobacter baumannii through one-step chromosomal gene inactivation. mBio 5:e01313-14–e01314. https://doi.org/10.1128/mBio.01313-14.
50. Bratu S, Landman D, Martin DA, Georgescu C, Quale J. 2008. Correlation of antimicrobial resistance with β-lactamases, the OmpA-like porin, and efflux pumps in clinical isolates of *Acinetobacter baumannii* endemic to New York City. Antimicrob Agents Chemother 52:2999–3005. https://doi.org/10.1128/aac.01684-07.
51. Iacono M, Villa L, Fortini D, Bordoni R, Imperi F, Bonnal RJP, Sicheritz-Ponten T, De Bellis G, Visca P, Cassone A, Carattoli A. 2008. Whole-genome pyrosequencing of an epidemic multidrug-resistant *Acinetobacter baumannii* strain belonging to the European clone II group. Antimicrob Agents Chemother 52:2616–2625. https://doi.org/10.1128/aac.01643-07.